Applied Surface Science 481 (2019) 421–432

Contents lists available at ScienceDirect

Applied Surface Science

journal homepage: www.elsevier.com/locate/apsusc

Full length article

Acetylene selective hydrogenation over different size of Pd-modified Cu cluster catalysts: Effects of Pd ensemble and cluster size on the selectivity and activity

Riguang Zhang, Mifeng Xue, Baojun Wang*, Lixia Ling

Key Laboratory of Coal Science and Technology of Ministry of Education and Shanxi Province, Taiyuan University of Technology, Taiyuan 030024, Shanxi, PR China

ARTICLE INFO

Keywords:
Cu-based catalyst
Pd ensemble
Cluster size
Acetylene selective hydrogenation
Selectivity
Activity

ABSTRACT

Aiming at identifying the effects of Pd ensemble and cluster size on the selectivity and activity of C_2H_2 selective hydrogenation over Pd-modified Cu nano-cluster catalysts, the catalytic performance of C_2H_2 selective hydrogenation over different cluster sizes of Pd-modified Cu catalyst with different Pd ensemble are examined using density functional theory calculations. A new evaluation method of the C_2H_4 selectivity is defined. The results indicate that the promoter Pd cannot improve C_2H_4 selectivity and activity over the small-sized Cu_{13} and the large-sized Cu_{55} clusters. Only when Cu catalyst has a moderate size such as Cu_{38} cluster, the Pd ensemble composed of outer shell with 6 coordination and its contiguous inner-layer Pd atoms can significantly improve C_2H_4 selectivity and activity. This study provides a theoretical clue for the design of highly efficient and cost-effective noble promoter-modified Cu-based catalysts by controlling the cluster size and the promoter ensemble for C_2H_2 selective hydrogenation.

1. Introduction

Ethylene (C_2H_4) as an important chemical raw materials is from the thermal cracking of petroleum fractions [1–4], however, a trace amount of acetylene (C_2H_2) impurity is produced, which can poison the catalyst of C_2H_4 polymerization [4–8]. Thus, the C_2H_2 impurity must be removed from C_2H_4 feedstock. C_2H_2 selective hydrogenation to C_2H_4 in the C_2H_4 feedstock is one of the most utilized methods to remove C_2H_2 impurity [4,9,10]. The noble-metal Pd catalyst has been widely used due to its good activity, however, it exhibits poor selectivity toward C_2H_4 formation [1,4,11,12], as a result, the second metal promoters such as Ag [4,13,14], Co [15,16], Cu [17–20], Ni [21–23] are doped into Pd to improve the selectivity toward C_2H_4 formation; Among them, Cu is the most advantageous promoter, it can significantly enhance the catalytic performance of C_2H_2 selective hydrogenation [17–20].

Recently, Pd-modified Cu-based catalyst have received extensive attention, which shows excellent C_2H_4 selectivity and activity compared to the single Cu and Pd catalysts [17,24–28]. In the Pd-modified Cu-based catalysts, the synergistic effect between Cu and Pd play a key role, the cost-effective Cu can inhibit the hydrogenation of C_2H_4 to by-product ethane, and presents high C_2H_4 selectivity at higher temperature (above 440 K) [17,19,29,30], the noble metal Pd is the main active component to show good activity of C_2H_4 formation. For example, Kyriakou et al. [24] suggested that the modification of Cu catalyst by isolated Pd atom significantly improve the selectivity of C_2H_4 for C_2H_2 selective hydrogenation. McCue et al. [17] experimentally show that Pd-modified Cu/Al_2O_3 catalyst with larger Cu: Pd ratio (50: 1) presents excellent selectivity and activity for C_2H_2 selective hydrogenation. Therefore, Pd-modified Cu-based catalyst is of great significance to improve the catalytic performance of C_2H_2 selective hydrogenation.

On the other hand, the heterogeneous catalysts usually exist in the mixture form of different size distribution of metal particles, in which only the metal particles with a suitable size distribution can perform as catalytic active species, whereas other-size particles are either inert or may trigger undesired side reactions [31–35]. Nowadays, many studies showed that the particle size of the catalyst affect its catalytic performance. For example, Liu et al. [31] show that the dissociation barrier of H_2 present the trend of U-type with the increasing of Pd_n (n = 4, 6, 13, 19, 55) cluster size, Pd_{13} cluster with the moderate size has the highest activity toward H_2 dissociation. The experiments by Karelovic et al. [32] found that Cu cluster with larger size are beneficial to prevent the formation of by-product CO of CO_2 hydrogenation to methanol, enhance the selectivity and activity toward CH_3OH. Zuo et al. [33] investigated the catalytic performance of different sizes of Cu catalyst for methanol decomposition reaction, confirming that compared with the larger size Cu(111) surface, the smaller cluster (Cu_{29} and Cu_{69}) can

* Corresponding author at: No. 79 Yingze West Street, Taiyuan 030024, PR China.
E-mail address: wangbaojun@tyut.edu.cn (B. Wang).

https://doi.org/10.1016/j.apsusc.2019.03.006
Received 20 December 2018; Received in revised form 26 February 2019; Accepted 1 March 2019
Available online 02 March 2019
0169-4332/

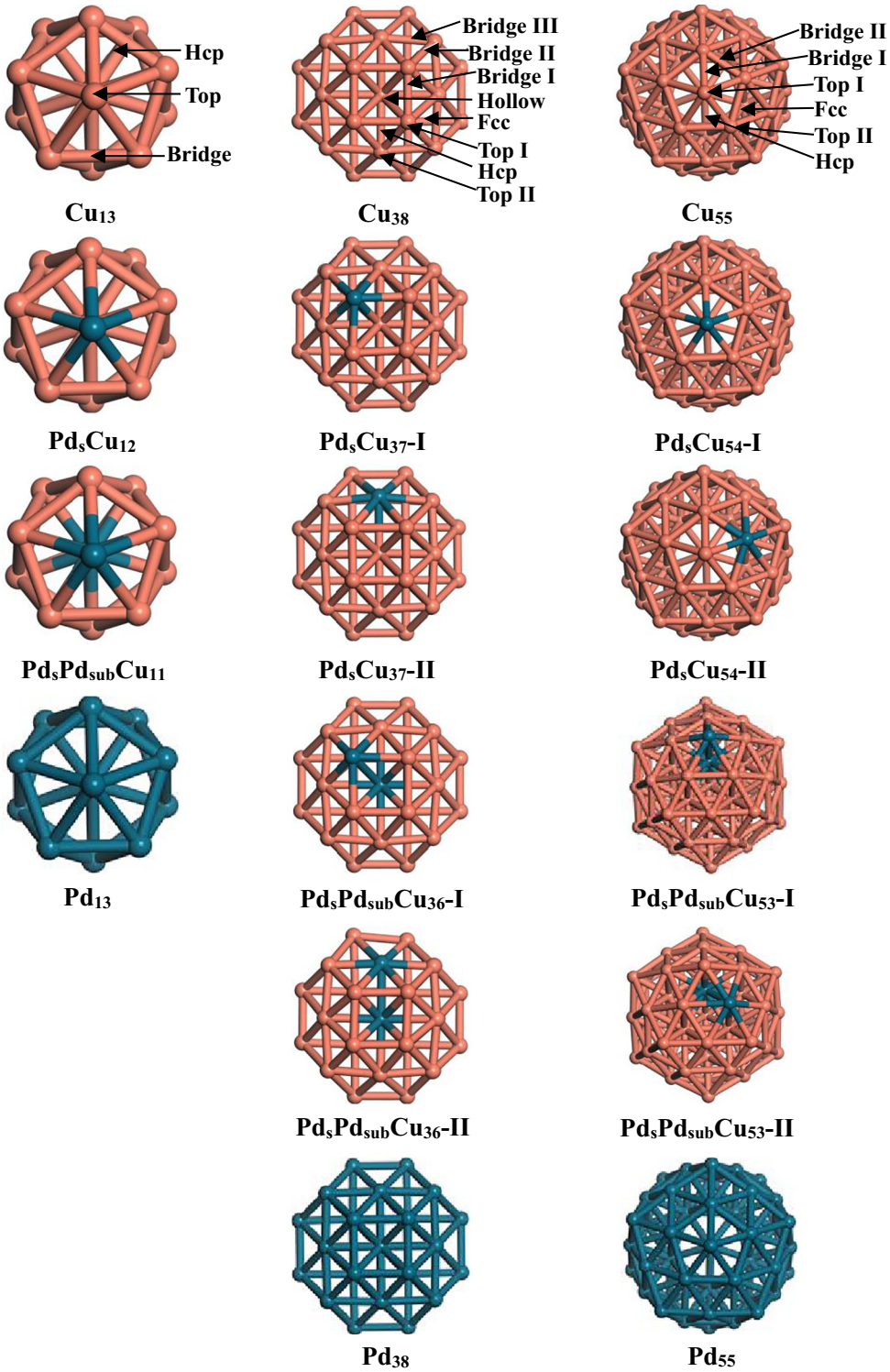

Fig. 1. The optimized structures for different sizes of single Cu clusters, Pd-modified Cu clusters and single Pd clusters.

decrease the energy barrier of methanol and formaldehyde dehydrogenation, and inhibit the desorption of by-product formaldehyde. Zhang et al. [34] demonstrated that Rh_4 cluster can achieve excellent catalytic performances than the larger size Rh(111) surface for syngas conversion to C_2 species. Zhao et al. [35] suggested that the size of the single Cu catalysts has important effects on the catalytic performance of C_2H_2 selective hydrogenation, it affects the choice of the most optimal pathway, which affects the C_2H_4 selectivity latter; the larger size of Cu_{55} cluster enhances the selectivity toward gaseous C_2H_4 formation. Up to now, to the best of our knowledge, as for the Pd-modified Cu-based catalysts, the effects of the catalyst size on the catalytic performance for C_2H_2 selective hydrogenation are still unclear.

For the Pd-modified Cu-based catalyst, previous experiments [28,36] observed that a trace amount of Pd atom can penetrate into the subsurface of Cu(111) during the deposition process, suggesting that both the surface and subsurface Pd atoms exhibit in the alloy systems; Thus, in this study, we turn our attention on two types of the structures, one is that with the individual Pd atom at the surface; the other is Pd

Table 1
The adsorption (G_{ads}) and activation free energy (ΔG_a) of C_2H_4 hydrogenation, as well as C_2H_4 selectivity (ΔG_{sel}) over three types of Pd-modified Cu_{55} clusters obtained using different functional (GGA-PBE, GGA-PW91 and GGA-BLYP) at 520 K.

Clusters	GGA-PBE			GGA-PW91			GGA-BLYP		
	ΔG_a	G_{ads}	ΔG_{sel}	ΔG_a	G_{ads}	ΔG_{sel}	ΔG_a	G_{ads}	ΔG_{sel}
Pd_sCu_{54}-I	101.2	−119.3	−18.1	113.1	−129.3	−16.2	68.6	−83.9	−15.3
$Pd_sPd_{sub}Cu_{53}$-I	77.7	−117.7	−40.0	110.0	−130.1	−20.1	61.8	−97.1	−35.3
$Pd_sPd_{sub}Cu_{53}$-II	113.3	−100.5	12.8	114.8	−104.2	10.6	113.7	−104.6	9.1

Table 2
Adsorption free energies of C_2H_x(x = 2–5) species at 520 K on different sizes of the single Cu, Pd-modified Cu, and the single Pd clusters.

Clusters	Adsorption free energies (G_{ads}/kJ·mol^{-1})				
	C_2H_2	C_2H_3	C_2H_4	$CHCH_3$	C_2H_5
Cu_{13}	−251.5	−331.6	−128.9	−250.4	−255.4
Pd_sCu_{12}	−241.4	−411.8	−136.7	−439.1	−256.9
$Pd_sPd_{sub}Cu_{11}$	−224.3	−329.4	−139.1	−414.1	−275.4
Pd_{13}	−198.6	−311.6	−117.9	−403.8	−224.1
Cu_{38}	−196.3	−310.9	−95.6	−381.6	−238.7
Pd_sCu_{37}-I	−186.3	−319.5	−98.5	−398.1	−269.3
Pd_sCu_{37}-II	−172.4	−331.0	−88.9	−421.4	−259.9
$Pd_sPd_{sub}Cu_{36}$-I	−192.0	−334.3	−106.0	−427.8	−269.5
$Pd_sPd_{sub}Cu_{36}$-II	−183.5	−302.7	−83.9	−360.3	−245.7
Pd_{38}	−244.6	−402.0	−166.3	−472.3	−295.3
Cu_{55}	−174.5	−298.3	−103.0	−385.9	−245.1
Pd_sCu_{54}-I	−209.1	−327.1	−119.3	−426.5	−265.8
Pd_sCu_{54}-II	−204.6	−333.4	−113.7	−375.2	−277.7
$Pd_sPd_{sub}Cu_{53}$-I	−177.5	−292.8	−117.7	−368.2	−200.9
$Pd_sPd_{sub}Cu_{53}$-II	−178.2	−254.5	−100.5	−368.9	−217.4
Pd_{55}	−295.6	−396.6	−189.2	−487.6	−301.6

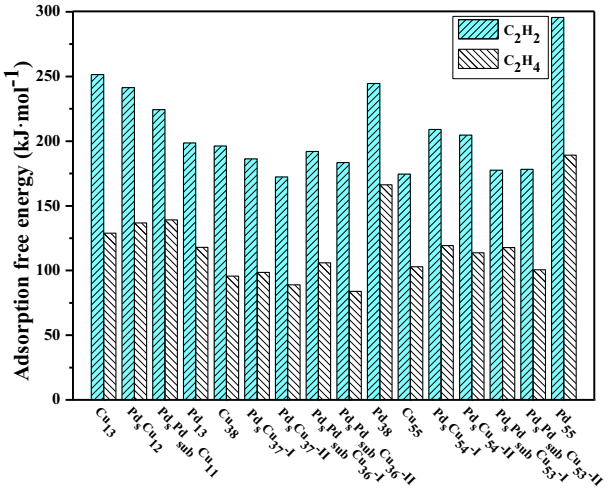

Fig. 2. The adsorption free energies of C_2H_2 and C_2H_4 over different sizes of the single Cu, Pd-modified Cu and the single Pd catalysts.

ensemble consisted of Pd atoms at both surface and its contiguous subsurface. Especially for the ensemble effect, Duan et al. [37] indicated that the Pt ensemble over Pt-modified Au(111) surface effectively enhanced the catalytic activity toward HCOOH oxidation, and prevent the formation of by-product CO. Yuan and Liu [38] confirmed that the small Pd ensemble over Pd-modified Au(111) surface is highly efficient for HCOOH oxidation to CO_2 instead of CO. Fu and Luo [39] revealed that the Pd ensemble formed by Pd atoms at the surface and joint subsurface of Cu(111) are beneficial to improve the catalytic activity of H_2 dissociation, this type of Pd ensemble is also the active center for C_2H_2 selective hydrogenation [28], which effectively improve the C_2H_4 selectivity and activity. Yet, the effect of Pd ensemble in different size of Pd-modified Cu-based catalysts on the C_2H_4 selectivity and activity in C_2H_2 selective hydrogenation is still unknown.

In this study, to elucidate the effects of Pd ensemble and size effects on C_2H_4 selectivity and activity, the mechanism of C_2H_2 selective hydrogenation on different sizes of Pd-modified Cu-based catalysts were examined; here, the density functional theory (DFT) calculations are employed. Moreover, different sizes of Pd-modified Cu clusters are selected to represent different sizes of Pd-modified Cu-based catalyst to achieve the effect of the catalyst size, moreover, compared to the individual Pd atom, different types of Pd ensemble consisted of the outer shell and its contiguous inner shell Pd atoms are considered to obtain the effect of Pd ensemble. It is hoped that our results can give a theoretical guidance to modifying Cu-based catalysts in industry.

2. Calculation methods and models

2.1. Calculation methods

In this study, all calculations were carried out using density functional theory (DFT) in Dmol^3 program package [40,41], the generalized gradient approximation (GGA-PBE) [42,43] was employed for the exchange correlation effects. The DNP was selected to expand the valence electron functions, the ECP [44] and all-electron basis set are used for Pd-doped Cu-based catalysts and small molecules, respectively. Moreover, the approach for searching the transition states is the complete LST/QST method. Further, the imaginary frequency and TS confirmation were performed to confirm the transition state [45,46].

Previous studies [17,47] have shown that the formation of green oil in C_2H_2 selective hydrogenation can be inhibited by regulating the reaction conditions, such as higher H_2/C_2H_2 ratio and reaction temperature. Thus, a higher H_2/C_2H_2 ratios with 10:1 and higher temperature with 520 K are choose in this paper, namely, the effects of green oil is ignored. Moreover, the pressures of H_2, C_2H_2, and C_2H_4 are set to be 0.1, 0.01, and 0.89 atm based on the realistic experiment conditions [47,48].

The adsorption free energy (G_{ads}) is calculated by the Eq. (1):

$$G_{ads} = E_{elec}(\text{all}) + G_m^{\theta}(\text{all}) - (E_{elec}(\text{mol}) + G_m^{\theta}(\text{mol}) + E_{elec}(\text{sub}) + G_m^{\theta}(\text{sub})) \quad (1)$$

As shown in the Eq. (1), E_{elec}(all) represents the total energy of the adsorbate-substrate system, E_{elec}(mol) and E_{elec}(sub) represents the energy of gaseous molecule and the cluster catalyst, respectively. $G_m{}^{\theta}$(mol), $G_m{}^{\theta}$(sub) and $G_m{}^{\theta}$(all) correspond to the Gibbs free energy of gaseous molecule, the cluster, and the adsorbed system at 520 K.

The activation free energy ($\Delta_r{}^{\neq}G_m{}^{\theta}$) and reaction free energy ($\Delta_rG_m{}^{\theta}$) of the elementary reactions at 520 K occurred on Pd-modified Cu cluster catalyst are calculated on the basis of the Eqs. (2) and (3) [49].

$$\Delta_r^{\neq}G_m^{\theta} = (E_{elec}(\text{TS}) - E_{elec}(\text{R})) + (G_m^{\theta}(\text{TS}) - G_m^{\theta}(\text{R})) \quad (2)$$

$$\Delta_rG_m^{\theta} = (E_{elec}(\text{P}) - E_{elec}(\text{R})) + (G_m^{\theta}(P) - G_m^{\theta}(R)) \quad (3)$$

where E_{elec}(TS), E_{elec}(R) and E_{elec}(P) are the electron energies of transition state, reactant and product, respectively. $G_m{}^{\theta}$(TS), $G_m{}^{\theta}(R)$ and

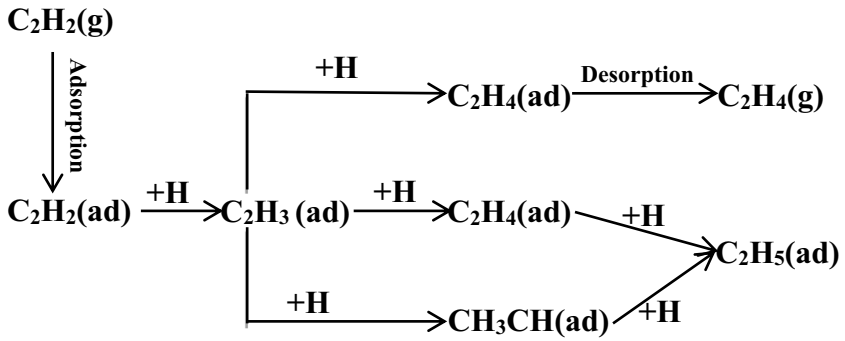

Fig. 3. The reaction pathways of C_2H_2 selective hydrogenation.

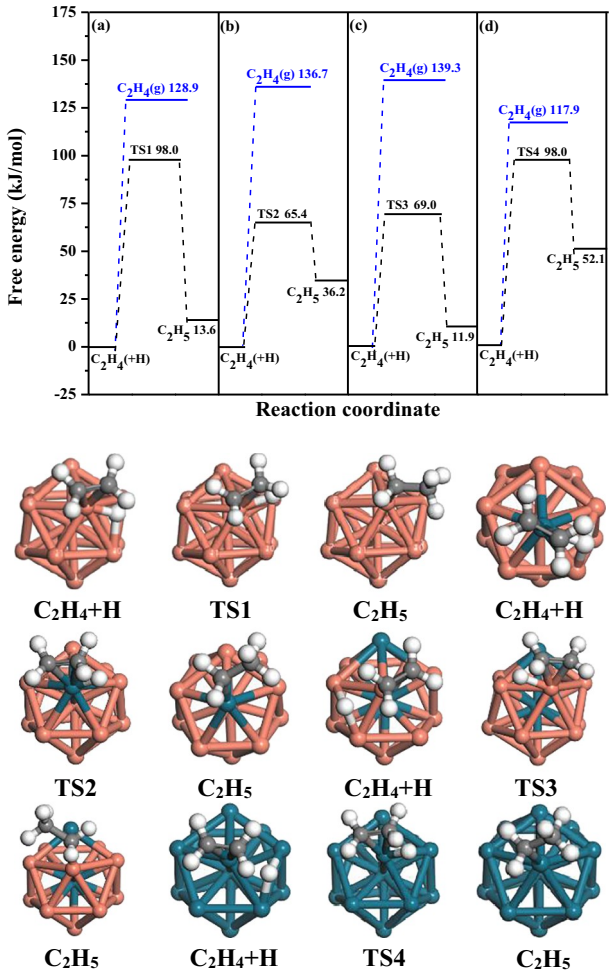

Fig. 4. The potential energy profile for the C_2H_4 hydrogenation and C_2H_4 desorption over the (a) single Cu_{13}, (b) Pd_sCu_{12}, (c) $Pd_sPd_{sub}Cu_{11}$ and (d) single Pd_{13} clusters.

$G_m^{\theta}(P)$ are the corresponding corrections for the standard free energies at a finite temperature (520 K). E_{elec}(R) and E_{elec}(P) can be obtained from a geometry optimization of reactant and product, while E_{elec}(TS) can be calculated from TS search using DMol[3]. On the other hand, once the structures of transition state, reactant and product are determined, the results from a vibrational analysis calculation can be used to compute important thermodynamic properties, such as enthalpy (H), entropy (S), free energy (G) and heat capacity at constant pressure (C_p) as a function of temperature. In our calculation, the values of G_m^{θ}(TS), $G_m^{\theta}(R)$ and $G_m^{\theta}(P)$ at a finite temperature (520 K) can be directly obtained from the data in DMol[3] output document of frequency analysis which have included the contribution of the entropy term.

2.2. Calculation models

In this paper, the single Cu catalyst with different sizes is represented by three Cu clusters with different diameters (5, 8 and 10 Å for 13, 38 and 55 clusters, respectively.) Based on these clusters, a series of Pd-modified Cu-based catalysts are formed by replacing Cu atoms of outer shell and its contiguous inner shell with Pd atoms, which can present different sizes of Pd-modified Cu-based catalyst and different types of Pd ensemble. Fig. 1 shows all structures for different sizes of Pd-modified Cu clusters.

As shown in Fig. 1, Cu_{13} cluster with icosahedron structure is the smallest magic cluster for Cu clusters, which composed of twenty (111) facets with an outer shell includes 12 Cu atoms as well as a Cu atom as the core [35,50–53]. All the Cu atoms located on the outer shell are equivalent due to same coordination number, thus, there is only one case for one Cu atom replaced by Pd atom in the outer shell of Cu_{13} cluster (named as Pd_sCu_{12}), subsequently, there is also one case with one inner Cu atom replaced by Pd atom in the core of Pd_sCu_{12} (named as $Pd_sPd_{sub}Cu_{11}$). Three adsorption sites exist.

For Cu_{38} cluster, previous studies [54–57] have demonstrated that the most stable structure among all isomers is the truncated octahedron structure. Different from Cu_{13} cluster, the inner shell of Cu_{38} cluster is an octahedron structure including 6 Cu atoms, the outer shell includes 32 atoms composed of (111) and (100) facets, and there are two different coordination numbers of Cu atoms in the outer shell (6 and 9, respectively); accordingly, a Cu atom replaced by a Pd atom in the outer shell of Cu_{38} cluster have two structures named as Pd_sCu_{37}-I and Pd_sCu_{37}-II. Based on Pd_sCu_{37}-I and Pd_sCu_{37}-II clusters, two structures of Pd ensembles consisted of the outer shell and its contiguous inner core Pd atoms are denoted as $Pd_sPd_{sub}Cu_{36}$-I and $Pd_sPd_{sub}Cu_{36}$-II, respectively. Based on 6 and 9-coordination atoms of the outer shell, there are eight different adsorption sites.

Cu_{55} cluster with the I_h symmetry is the most stable structure among all the isomers [58–61], the outer shell consists of 20 (111) facets by 42 Cu atoms, and the Cu_{13} cluster is the core shell. There are two different coordination numbers of Cu atoms over the outer shell numbers (6 and 8, respectively). As a result, there are two structures that a Cu atom replaced by a Pd atom in the outer shell (Pd_sCu_{54}-I and Pd_sCu_{54}-II); accordingly, two structures correspond to Pd ensembles consisted of the outer shell and its contiguous sub-layer Pd atoms, which are called as $Pd_sPd_{sub}Cu_{53}$-I and $Pd_sPd_{sub}Cu_{53}$-II, respectively. Based on 6 and 8-coordination atoms on the outer shell of Pd-doped Cu_{55} cluster, six different adsorption sites are formed.

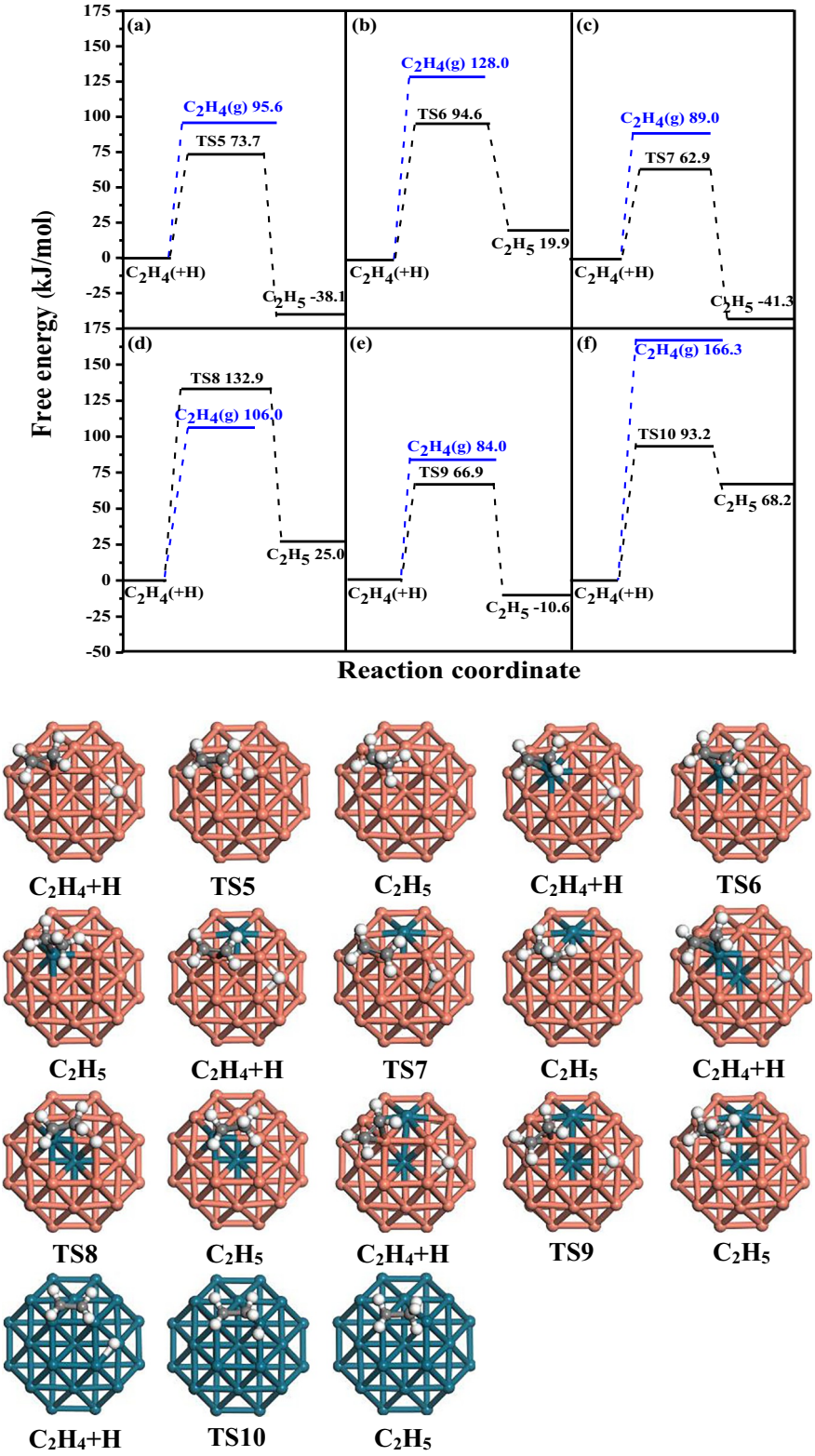

Fig. 5. The potential energy profile for C_2H_4 hydrogenation and C_2H_4 desorption over (a) single Cu_{38}, (b) Pd_sCu_{37}-I, (c) Pd_sCu_{37}-II, (d) $Pd_sPd_{sub}Cu_{36}$-I, (e) $Pd_sPd_{sub}Cu_{36}$-II, (f) single Pd_{38} clusters.

Further, different sizes of pure Pd catalyst are also considered, C_2H_2 selective hydrogenation on the pure Pd_{13}, Pd_{38} and Pd_{55} clusters (see Fig. 1) are examined as the references to clarify the selectivity and activity of the single Cu and Pd-modified Cu clusters toward C_2H_2 selective hydrogenation.

3. Results and discussion

3.1. Reliability evaluation of calculation methods

Firstly, since the hydrogenation and desorption of C_2H_4 are the key

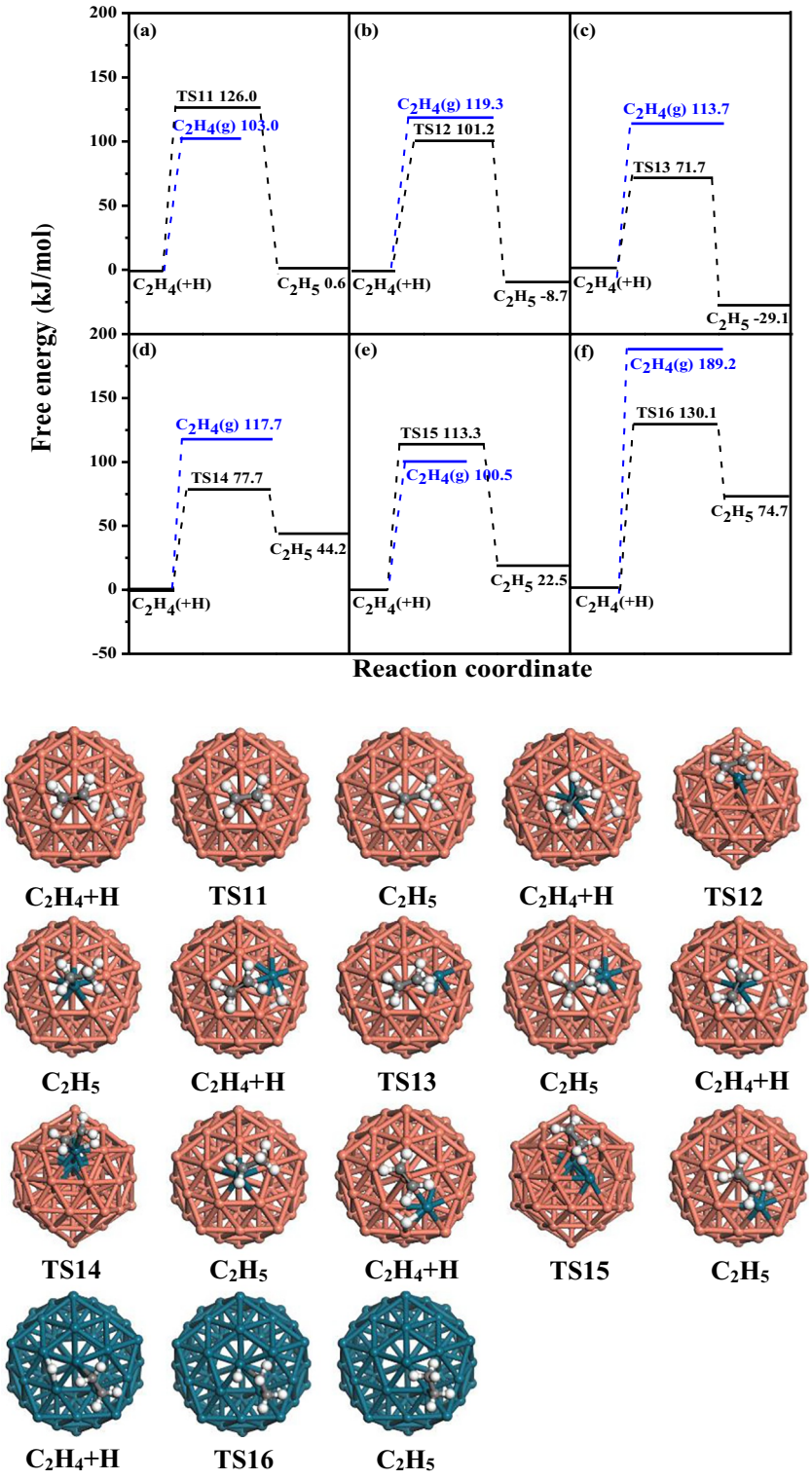

Fig. 6. The potential energy profile for C_2H_4 hydrogenation and C_2H_4 desorption over (a) single Cu_{55}, (b) Pd_sCu_{54}-I, (c) Pd_sCu_{54}-II; (d) $Pd_sPd_{sub}Cu_{53}$-I; (e) $Pd_sPd_{sub}Cu_{53}$-II; (f) single Pd_{55} clusters.

steps to evaluate C_2H_4 selectivity in the selective hydrogenation of acetylene, different calculation functional (GGA-PBE, GGA-PW91 and GGA-BLYP) have been employed to calculate the activation free energies corresponding to the hydrogenation and desorption of C_2H_4 over a series of Pd-modified Cu clusters, as listed in Table 1, the results show that the selectivity of C_2H_4 over Pd_sCu_{54}-I cluster are -18.1, -16.2 and -15.3 kJ·mol^{-1} calculated by the GGA-PBE, GGA-PW91 and GGA-BLYP functional, respectively, suggesting that the Pd_sCu_{54}-I cluster exhibits poor C_2H_4 selectivity irrespective of the used calculation functional. Moreover, the $Pd_sPd_{sub}Cu_{53}$-I and $Pd_sPd_{sub}Cu_{53}$-II clusters shows the same results with Pd_sCu_{54}-I cluster, which means that the calculation results obtained from GGA-PBE functional is reliable to qualitatively evaluate C_2H_4 selectivity in the selective hydrogenation of C_2H_2 over Pd-modified Cu-based bimetallic catalysts. Secondly, our

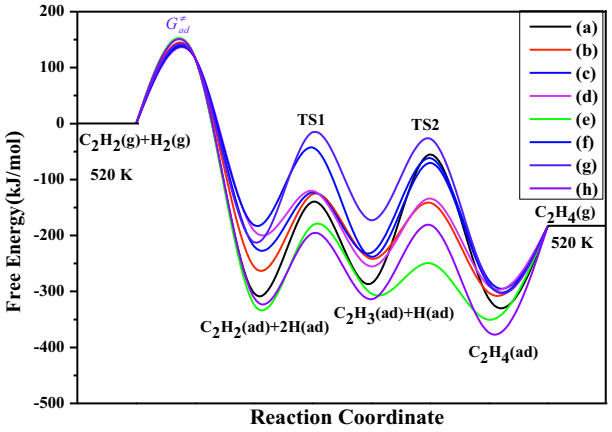

Fig. 7. Free energy profiles for the selective hydrogenation of C_2H_2 to C_2H_4 on different size of Pd-modified Cu clusters: (a) single Cu_{13}, (b) single Pd_{13}, (c) single Cu_{38}, (d) $Pd_sPd_{sub}Cu_{36}$-I, (e) single Pd_{38}, (f) single Cu_{55}, (g) $Pd_sPd_{sub}Cu_{53}$-II, (h) single Pd_{55}, respectively. The corresponding structures are shown in Fig. 8.

calculation results obtained from GGA-PBE functional can well illustrate that a small amount of promoter Pd-modified Cu cluster catalyst can improve the catalytic activity and selectivity of C_2H_4 formation in the selective hydrogenation of C_2H_2, which is in agreement with the reported experimental results. For instance, Kyriakou et al. [24] demonstrated that a very small quantity of individual Pd atoms in Cu surface can substantially lower the energy barrier of H_2 dissociation. McCue et al. [17] and Cao et al. [62] suggested that the modification of a trace amount of promoter Pd for Cu catalyst significantly improve the catalytic activity and selectivity of C_2H_4 formation in the selective hydrogenation of C_2H_2, which is consistent with our results. Thirdly, our calculation results obtained from GGA-PBE functional suggested that the ensemble composed of surface Pd and its contiguous subsurface Pd atoms in the Pd-modified Cu cluster catalysts can significantly improve the activity and selectivity of C_2H_4 formation in the selective hydrogenation of C_2H_2, which is in accordance with the theoretical calculation results by Fu and Luo [39] and Zhang et al. [28] over the Pd-modified Cu(111) periodic surfaces, which demonstrated that the Pd ensemble composed of the surface and contiguous subsurface atoms can significantly reduce the energy barrier of H_2 dissociation, furthermore significantly improve the catalytic activity and selectivity for C_2H_2 selective hydrogenation.

On the basis of above analysis, our calculation method using the GGA-PBE functional is reliable to qualitatively evaluate the catalytic performance of the promoter Pd-modified Cu cluster catalysts in the selective hydrogenation of C_2H_2.

3.2. The adsorption of C_2H_2 and C_2H_4

In the industry process of C_2H_2 selective hydrogenation, there are only about 0.1–1% C_2H_2, while the content of C_2H_4 is above 89% [28,35]. Thus, C_2H_2 on the catalyst must have the stronger adsorption ability than C_2H_4; as a result, the C_2H_2 impurities can be effectively removed from C_2H_4 feedstock. The adsorption free energies of C_2H_2 and C_2H_4 are listed in Table 2 and Fig. 2 (the corresponding stable adsorption configurations are presented in Fig. S1); On Pd-modified Cu_{13} clusters, the stable adsorption configuration of C_2H_2 is the η^2-η^2 model on the "3-fold hollow" site, which is consistent with the previous results [35]. For the Pd-modified Cu_{38} and Cu_{55} clusters, the most stable adsorption site is the "4-fold diagonal hollow" site for C_2H_2. For C_2H_4 species, it is adsorbed at the low-coordination top sites on all clusters with the same adsorption configurations. In addition, the stable adsorption configurations of C_2H_3, $CHCH_3$ and C_2H_5 species are also shown in Fig. S1.

As shown in Fig. 2, the adsorption of C_2H_2 over all clusters are much stronger than that of C_2H_4, which means that a trace amount of C_2H_2 in C_2H_4 feedstock can be stably adsorbed on the catalyst, and therefore facilitate the C_2H_2 hydrogenation.

3.3. The evaluation method of the selectivity of C_2H_2 selective hydrogenation

As shown in Fig. 3, three potential pathways exist, *C_2H_4 desorption pathway*, *C_2H_4 intermediate pathway* and *$CHCH_3$ intermediate pathway*. In order to achieve excellent C_2H_4 selectivity, the C_2H_4 desorption pathway should be promoted; whereas both C_2H_4 and $CHCH_3$ intermediate pathways should be suppressed.

In this study, a new evaluation method of the C_2H_4 selectivity is proposed, the preference between the hydrogenation and desorption of C_2H_4 is first considered, if C_2H_4 is prefer to desorption rather than hydrogenation, we need to further examine $CHCH_3$ intermediate pathway, which may affect the C_2H_4 selectivity. On the contrary, if the C_2H_4 intermediate pathway is more favorable than C_2H_4 desorption pathway, the catalyst exhibits poor C_2H_4 selectivity, and the $CHCH_3$ intermediate pathway on the C_2H_4 selectivity are not be considered.

According to previous studies [63–65], the adsorption free energy of C_2H_4 is used to represent the desorption free energy. Recently, Xu et al. [66] have defined a descriptor of C_2H_4 selectivity using the Gibbs free energy difference (ΔG) between C_2H_4 hydrogenation and its desorption energy, where a larger ΔG indicates higher C_2H_4 selectivity. Thus, the C_2H_4 selectivity in this study is described by the energy differences between C_2H_4 hydrogenation (ΔG_a) and C_2H_4 desorption ($|G_{ads}|$), which is defined as ΔG_{sel} in the Eq. (4):

$$\Delta G_{sel} = \Delta G_a - |G_{ads}| \quad (4)$$

The positive ΔG_{sel} represents C_2H_4 prefers to desorption from catalyst rather than hydrogenation, and exhibits good C_2H_4 selectivity.

3.4. C_2H_2 hydrogenation on Pd-modified Cu_{13} clusters

On the single Cu_{13} cluster, as shown in Fig. 4(a), the adsorption free energy of C_2H_4 is higher than that of C_2H_4 hydrogenation to C_2H_5 (128.9 *vs.* 98.0 kJ·mol^{-1}), suggesting that the C_2H_4 intermediate pathway is more favorable than C_2H_4 desorption pathway, namely, the single Cu_{13} cluster exhibits poor C_2H_4 selectivity with the ΔG_{sel} of −30.9 kJ·mol^{-1}. For the Pd-modified Cu_{13} clusters, as shown in Fig. 4(b) and (c), the adsorption free energies of C_2H_4 are much higher than those of C_2H_4 hydrogenation, namely, both Pd_sCu_{12} and $Pd_sPd_{sub}Cu_{12}$ clusters show poor selectivity of C_2H_4 with the ΔG_{sel} of −71.3 and −70.3 kJ·mol^{-1}, respectively. On the single Pd_{13} cluster (Fig. 4(d)), C_2H_4 hydrogenation to C_2H_5 is more preferable than its desorption to C_2H_4 gaseous (98.0 *vs.* 117.9 kJ·mol^{-1}), suggesting that C_2H_4 intermediate pathway is more favorable than C_2H_4 desorption pathway, thus, the single Pd_{13} cluster exhibits poor C_2H_4 selectivity with the ΔG_{sel} of −19.9 kJ·mol^{-1}.

As mentioned above, on the single Cu_{13}, Pd_{13}, and Pd-modified Cu_{13} clusters, the most optimal pathway is C_2H_4 hydrogenation pathway, namely, C_2H_4 is easier to be over-hydrogenated to ethane. Thus, the promoter Pd and its ensemble consisted of outer shell and its contiguous inner Pd atoms cannot improve C_2H_4 selectivity over all the Pd-modified Cu_{13} clusters.

3.5. C_2H_2 hydrogenation on Pd-modified Cu_{38} clusters

As shown in Fig. 5(a), on the single Cu_{38} cluster, the C_2H_4 intermediate pathway is more favorable than C_2H_4 desorption pathway (73.7 *vs.* 95.6 kJ·mol^{-1}), the C_2H_4 selectivity (ΔG_{sel}) is −21.9 kJ·mol^{-1}. Similarly, as shown in Fig. 5(b), (c) and (e), on the Pd_sCu_{37}-I, Pd_sCu_{37}-II and $Pd_sPd_{sub}Cu_{36}$-II clusters, C_2H_4 prefers to be hydrogenated to C_2H_5 rather than its desorption to gaseous C_2H_4, thus, these

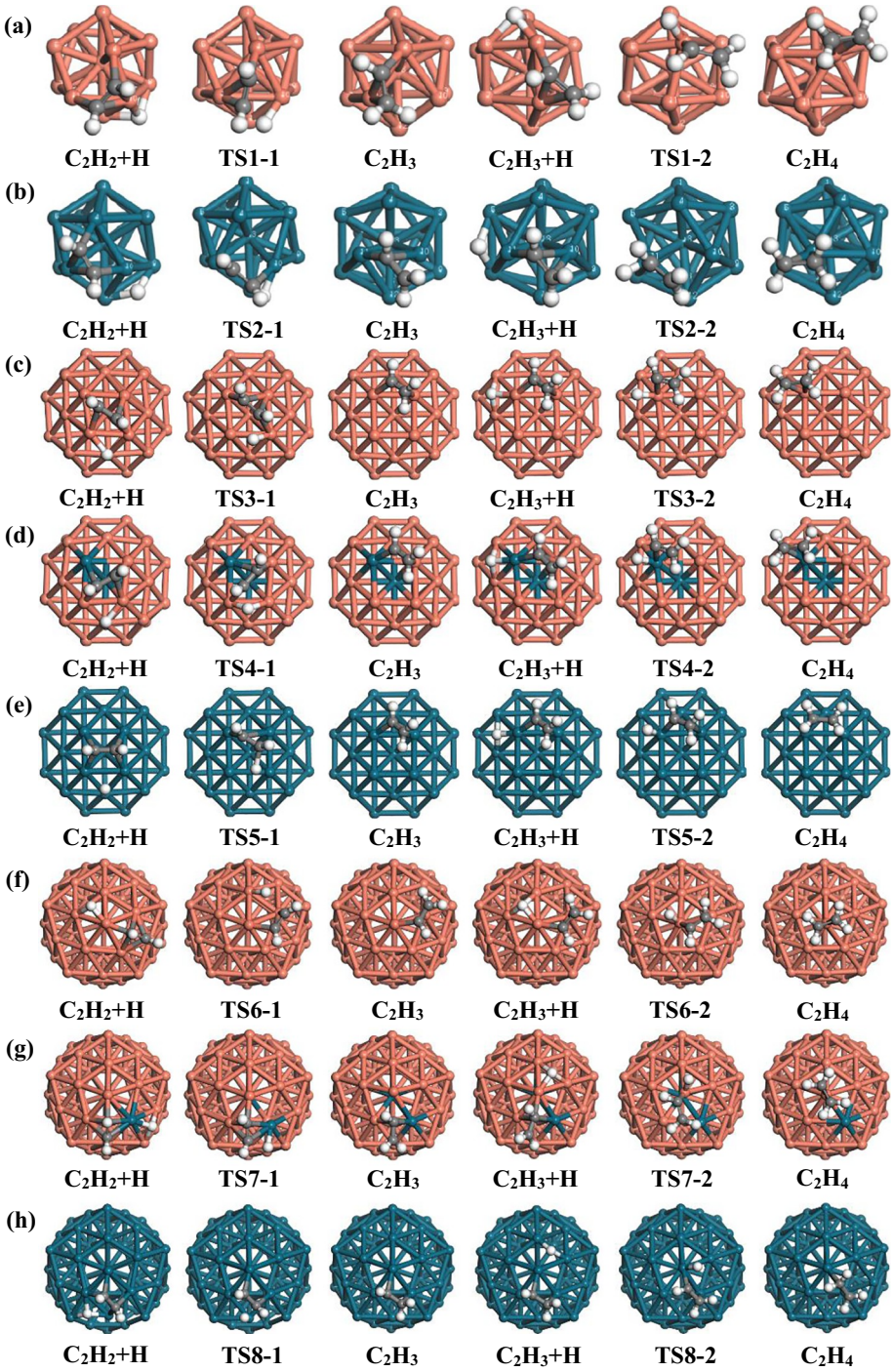

Fig. 8. The structures of reactants, transition states and products for C_2H_2 hydrogenation to C_2H_4 on different size of Pd-modified Cu clusters: (a) single Cu_{13}, (b) single Pd_{13}, (c) single Cu_{38}, (d) $Pd_sPd_{sub}Cu_{36}$-I, (e) single Pd_{38}, (f) single Cu_{55}, (g) $Pd_sPd_{sub}Cu_{53}$-II, (h) single Pd_{55}, respectively.

clusters shows poor C_2H_4 selectivity with the ΔG_{sel} of −33.4, −26.1 and −17.1 kJ·mol^{-1}, respectively. However, for the $Pd_sPd_{sub}Cu_{36}$-I cluster (Fig. 5(d)) C_2H_4 desorption is more advantageous than its hydrogenation (106.0 *vs.* 132.9 kJ·mol^{-1}), thus, $CHCH_3$ intermediate pathway is further considered (Fig. S2), starting from C_2H_3 intermediate, the overall free energy of $CHCH_3$ intermediate pathway is much higher than that of C_2H_4 desorption pathway (84.5 *vs.* 41.9 kJ·mol^{-1}), and C_2H_2 prefers to be hydrogenation to C_2H_4 rather than $CHCH_3$ intermediate; thus, the gaseous C_2H_4 is the main product over the $Pd_sPd_{sub}Cu_{36}$-I cluster, which presents better C_2H_4 selectivity with the ΔG_{sel} of 26.9 kJ·mol^{-1}. For the single Pd_{38} cluster, as shown in Fig. 5(f), C_2H_4 desorption is much difficult than C_2H_4 hydrogenation (166.3 *vs.* 93.2 kJ·mol^{-1}), thus, the single Pd_{38} cluster shows poor C_2H_4 selectivity with the ΔG_{sel} of −73.1 kJ·mol^{-1}.

On the basis of above analysis, for the Pd-modified Cu_{38} clusters, when the individual Pd atom is doped into the outer shell of Cu_{38} cluster to form Pd_sCu_{37}-I and Pd_sCu_{37}-II clusters, which cannot improve the C_2H_4 selectivity (−33.4 and −26.1 kJ·mol^{-1}) compared to the single Cu_{38} cluster (−21.9 kJ·mol^{-1}). Interestingly, when the Pd atom is doped into the inner shell of Pd_sCu_{37}-I and Pd_sCu_{37}-II clusters to form $Pd_sPd_{sub}Cu_{36}$-I and $Pd_sPd_{sub}Cu_{36}$-II clusters, in which the Pd ensemble composed of outer shell and its contiguous inner shell Pd atoms can

Table 3
The values of $G_R^{ad} - G_R^{de} + G_P^{de}$, G_P^{de} (kJ·mol^{-1}) and reaction rate (r/s^{-1}·site^{-1}) at 520 K on different clusters.

Clusters	$G_R^{ad} - G_R^{de} + G_P^{de}$	G_P^{de}	r
Cu_{13}	−55.1	247.1	1.63×10^{-12}
Pd_{13}	−126.3	128.6	1.30×10^{0}
Cu_{38}	−61.5	157.1	1.79×10^{-3}
$Pd_sPd_{sub}Cu_{36}$-I	−120.0	70.5	8.94×10^{5}
Pd_{38}	−181.9	140.3	8.71×10^{-2}
Cu_{55}	−42.8	138.1	1.45×10^{-1}
$Pd_sPd_{sub}Cu_{53}$-II	−15.5	196.1	2.16×10^{-7}
Pd_{55}	−180.9	129.0	1.19×10^{0}

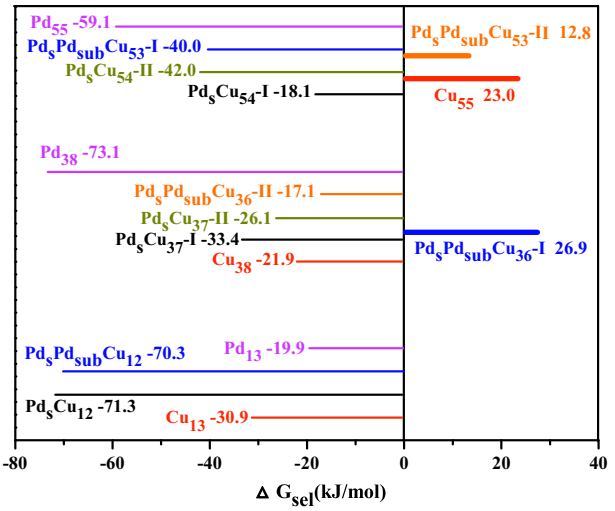

Fig. 9. The selectivity of C_2H_4 (ΔG_{sel}) over different sizes of the single Cu, Pd-modified Cu and the single Pd clusters at 520 K.

Table 4
The average Mulliken charges (e) of Pd and Cu atoms for different sizes of the single Cu, Pd-modified Cu and the single Pd clusters.

Cluster	Pd atoms	Cu atoms
Cu_{13}	–	−0.014
Pd_{13}	−0.032	–
Cu_{38}	–	−0.013
$Pd_sPd_{sub}Cu_{36}$-I	−0.196 (0.052)	0.004
Pd_{38}	−0.050	–
Cu_{55}	–	−0.023
$Pd_sPd_{sub}Cu_{53}$-II	−0.213 (−0.040)	0.004
Pd_{55}	−0.095	–

improve C_2H_4 selectivity (26.9 and −17.1 kJ·mol^{-1}), especially, the $Pd_sPd_{sub}Cu_{36}$-I cluster can substantially enhance C_2H_4 selectivity with the ΔG_{sel} of 26.9 kJ·mol^{-1}, namely, only the ensemble composed of outer shell Pd atom with 6 coordination and its joint inner shell Pd atoms can substantially improve the C_2H_4 selectivity for C_2H_2 selective hydrogenation.

3.6. C_2H_2 hydrogenation on Pd-modified Cu_{55} clusters

As shown in Fig. 6(a), on the single Cu_{55} cluster, C_2H_4 desorption is favorable than its hydrogenation (103.0 *vs.* 126.0 kJ·mol^{-1}); meanwhile, starting from C_2H_3 intermediate, the overall free energy of $CHCH_3$ intermediate pathway is higher than that of C_2H_4 desorption pathway (197.7 *vs.* 158.8 kJ·mol^{-1}) (Fig. S3). Thus, C_2H_4 desorption pathway is the most optimal, and the single Cu_{55} cluster exhibits good C_2H_4 selectivity with the ΔG_{sel} of 23.0 kJ·mol^{-1}.

On the Pd_sCu_{54}-I, Pd_sCu_{54}-II and $Pd_sPd_{sub}Cu_{53}$-I clusters, as shown in Fig. 6(b), (c) and (d), C_2H_4 intermediate pathway is more advantageous than C_2H_4 desorption pathway, therefore, these clusters shows poor C_2H_4 selectivity with the ΔG_{sel} of −18.1, −42.0 and −40.0 kJ·mol^{-1}, respectively. However, for the $Pd_sPd_{sub}Cu_{53}$-II cluster (Fig. 6(e)), C_2H_4 desorption pathway is advantageous than C_2H_4 intermediate pathway (100.5 *vs.* 113.3 kJ·mol^{-1}); moreover, starting from C_2H_3 intermediate, C_2H_4 desorption pathway is more preferred than $CHCH_3$ intermediate pathway (208.4 *vs.* 243.1 kJ·mol^{-1}, Fig. S4); thus, the $Pd_sPd_{sub}Cu_{53}$-II cluster exhibits good C_2H_4 selectivity with the ΔG_{sel} of 12.8 kJ·mol^{-1}. Further, as shown in Fig. 6(f), the single Pd_{55} cluster exhibits poor C_2H_4 selectivity with the ΔG_{sel} of −59.1 kJ·mol^{-1}.

In general, for the Pd-modified Cu_{55} clusters, the individual Pd atom doped into the outer shell (−18.1 and −42.0 kJ·mol^{-1}) and the ensemble composed of outer shell and its contiguous inner shell Pd atoms (−40.0 and 12.8 kJ·mol^{-1}) exhibit lower C_2H_4 selectivity compared to the single Cu_{55} cluster (23.0 kJ·mol^{-1}). Thus, introducing the promoter Pd into the Cu_{55} cluster cannot improve the selectivity of C_2H_4.

3.7. General discussion

According to above evaluation parameter of C_2H_4 selectivity, different sizes of Pd-modified Cu clusters with better C_2H_4 selectivity ($Pd_sPd_{sub}Cu_{36}$-I, Cu_{55} and $Pd_sPd_{sub}Cu_{53}$-II clusters) can be obtained, then, their corresponding catalytic activity of C_2H_4 formation are considered. In addition, C_2H_4 selectivity and activity over different sizes of the single Cu and Pd clusters are also investigated as a reference to obtain the role of Pd promoter and its ensemble in C_2H_2 selective hydrogenation over the Pd-modified Cu catalysts. The catalytic activity of C_2H_4 formation is described using the two-step model proposed by Hu et al. [67,68] (details in the Supplementary Materials), the reaction rates of C_2H_4 formation are calculated *via* the Eq. (5).

$$r = \frac{k_B T}{h} \frac{\left(1 - \frac{P_P}{P_R} e^{\frac{\Delta G}{RT}}\right)}{\frac{P^0}{P_R} e^{\frac{G_R^{ad} - G_R^{de} + G_P^{de}}{RT}} + e^{\frac{G_P^{de}}{RT}}} \quad (5)$$

According to the Eq. (5), the reaction rates of C_2H_4 formation is mainly depend on G_R^{ad}, G_R^{de}, and G_P^{de}, the values of G_R^{de} and G_P^{de}can be obtained by the free energy profiles of C_2H_2 selective hydrogenation to C_2H_4 (as shown in Figs. 7 and 8). Moreover, the value of G_R^{ad} is represented by the TS_R (R = C_2H_2, H_2), in this study, at the reaction temperature of T = 520 K, TS_{C2H2} = 117.6 kJ·mol^{-1} and TS_{H2} = 76.3 kJ·mol^{-1}, suggesting that C_2H_2 has higher adsorption free energy than H_2. Thus, the adsorption free energy of C_2H_2 (117.6 kJ·mol^{-1}) is selected as the limiting adsorption barrier of the reactants. Accordingly, the reaction rates of C_2H_4 formation on different sizes of Pd-modified Cu catalysts are calculated, as listed in Table 3.

3.7.1. The role of Pd promoter, the effects of Pd ensemble and cluster size on C_2H_4 selectivity and activity

As discussed above, for the Pd-modified Cu_{13} clusters, as shown in Fig. 9, the selectivity of C_2H_4 (ΔG_{sel}/kJ·mol^{-1}) follows the order: Pd_sCu_{12} (−71.3) < $Pd_sPd_{sub}Cu_{11}$ (−70.3) < Cu_{13} (−30.9) < Pd_{13} (−19.9), namely, C_2H_2 prefers to be over-hydrogenated to ethane, suggesting that the ways by introducing the promoter Pd into the small size of Cu_{13} cluster cannot improve the C_2H_4 selectivity compared to the single Cu_{13} cluster, as a result, the activity of C_2H_4 formation over Pd-modified Cu_{13} clusters is not considered. In addition, as listed in Table 3, the activity of C_2H_4 formation on the single Cu_{13} and Pd_{13} clusters are 1.63×10^{-12} and 1.30×10^{0} s^{-1}·site^{-1}, respectively, suggesting that the single Pd_{13} catalyst exhibits excellent catalytic activity compared to the single Cu_{13} catalyst for C_2H_2 selective hydrogenation, which agrees with previous studies [4–7].

For Pd-modified Cu_{38} clusters, as shown in Fig. 9, the C_2H_4 selectivity (ΔG_{sel}/kJ·mol^{-1}) follows the order: Pd_{38} (−73.1) < Pd_sCu_{37}-I (−33.4) < Pd_sCu_{37}-II (−26.1) < Cu_{38} (−21.9) < $Pd_sPd_{sub}Cu_{36}$-II

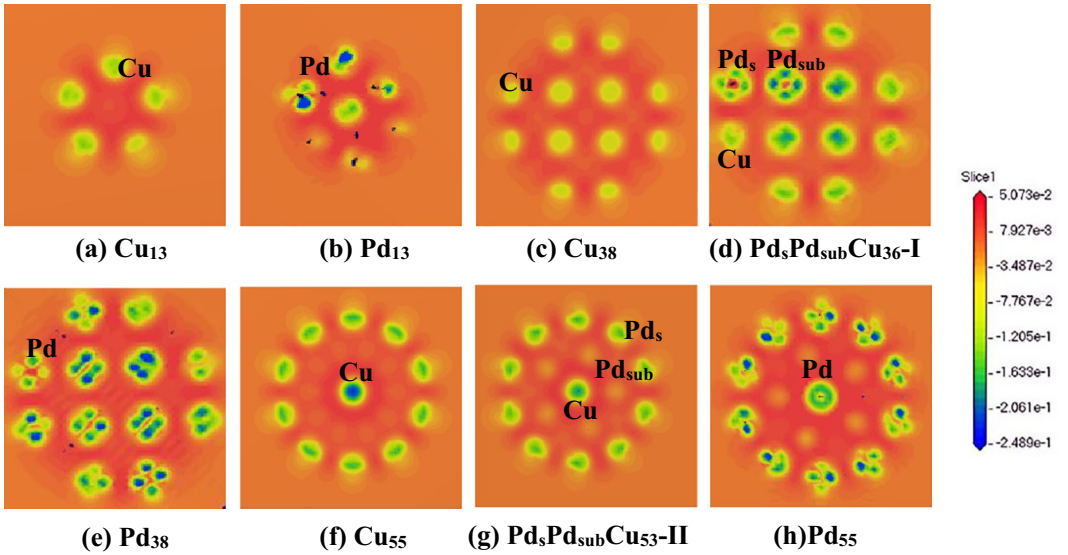

Fig. 10. Electron density difference contour maps of different size of Pd-modified Cu clusters: (a) single Cu_{13}, (b) single Pd_{13}, (c) single Cu_{38}, (d) $Pd_sPd_{sub}Cu_{36}$-I, (e) single Pd_{38}, (f) single Cu_{55}, (g) $Pd_sPd_{sub}Cu_{53}$-II, (h) single Pd_{55} cluster, respectively. Green represents the electron depletion regions, and orange represents the regions of electron accumulation.

(-17.1) < $Pd_sPd_{sub}Cu_{36}$-I (26.9), indicating that the individual Pd atom doped into the outer shell of Cu_{38} cluster cannot improve the C_2H_4 selectivity. However, $Pd_sPd_{sub}Cu_{36}$-I presents the better C_2H_4 selectivity, the corresponding activity (s^{-1}·$site^{-1}$) of C_2H_4 formation (8.94×10^5) is much higher than those of the single Cu_{38} and Pd_{38} clusters (1.79×10^{-3} and 8.71×10^{-2}). Namely, only the promoter Pd ensemble formed by outer shell and its contiguous inner shell Pd atoms can significantly enhance C_2H_4 selectivity and its formation activity.

For Pd-modified Cu_{55} clusters, the C_2H_4 selectivity (ΔG_{sel}/kJ·mol^{-1}) follows the order: Pd_{55} (-59.1) < Pd_sCu_{54}-II (-42.0) < $Pd_sPd_{sub}Cu_{53}$-I (-40.0) < Pd_sCu_{54}-I (-18.1) < $Pd_sPd_{sub}Cu_{53}$-II (12.8) < Cu_{55} (23.0). Moreover, as listed in Table 3, the sequence of catalytic activity (s^{-1}·$site^{-1}$) is: $Pd_sPd_{sub}Cu_{53}$-II (2.16×10^{-7}) < Cu_{55} (1.45×10^{-1}) < Pd_{55} (1.19×10^{0}). Thus, the Pd-modified Cu_{55} clusters exhibits poor C_2H_4 selectivity and activity compared to the single Cu_{55} and Pd_{55} cluster, namely, the ways by introducing the promoter Pd into the larger size of Cu_{55} cluster is invalid to improve the selectivity and activity of C_2H_4.

Based on above analysis, for the Pd-modified Cu catalyst, the ways by an individual Pd atom replacing an outer shell Cu atom cannot improve the catalytic performance of Cu catalysts; Moreover, the promoter Pd over the small-sized Cu_{13} and the large-sized Cu_{55} clusters cannot improve the activity and selectivity toward C_2H_4 formation. Only when the size of Pd-modified Cu catalyst is at a moderate-size such as Cu_{38} cluster, the Pd ensemble composed of outer shell with 6 coordination and the joint inner shell Pd atoms significantly improve the selectivity and activity of C_2H_4 in comparison with the single Cu and Pd catalysts. Thus, the moderate-size Pd-modified Cu catalyst with the Pd ensemble composed of inner shell and its contiguous inner shell Pd atoms is an efficient way to improve catalytic performance of C_2H_2 selective hydrogenation.

3.7.2. The analysis of electronic properties

Previous studies [69–72] have demonstrated that the electronic properties of the catalyst can affect the adsorption and catalytic performance, Han et al. [70] investigated the catalytic performance of Pd_mAg_n (m + n = 2–5) clusters supported on the defective anatase TiO_2 for C_2H_2 selective hydrogenation, suggesting that compared to the single Pd cluster, the modification of Ag changes the electronic states of Pd atoms, and weaken the adsorption ability of both C_2H_2 and C_2H_4, and therefore, improve the catalytic performance of C_2H_2 selective hydrogenation. In this study, the Mulliken charge distributions and the electron density difference of Pd-modified Cu clusters are presented in Table 4 and Fig. 10, respectively.

On the single Cu_{13} and Pd_{13} clusters, the charge of the outer atoms is uniformly distributed, and the average charge of Pd atoms for Pd_{13} cluster (-0.032 *e*) is more negative than that of Cu atoms (-0.014 *e*). Similarly, the electron density difference in Fig. 10(a) and (b) shows that the electron accumulation at the region of Pd atoms is more than that of Cu atoms, as a result, the single Pd_{13} cluster exhibits better activity of C_2H_4 formation than the single Cu_{13} cluster.

On the single Cu_{38} and Pd_{38} clusters, the charge of 6-coordinate outer shell Cu and Pd atoms are -0.013 and -0.050 *e*, respectively, which is more negative than that of 9-coordinate Cu and Pd atoms (-0.001 and 0.033 *e*), as a result, the 6-coordinate Cu and Pd atoms is the active center, which agrees with above kinetic results. As shown in Fig. 10(c) and (e), the charge density of Pd-Pd atoms are stronger than that of Cu-Cu atoms, thus, the single Pd_{38} cluster shows better activity of C_2H_4 formation than the single Cu_{38} cluster. Interestingly, for the $Pd_sPd_{sub}Cu_{36}$-I cluster, the charges of Pd atoms on the outer shell (-0.196 *e*) is more negative than that of the single Cu_{38} and Pd_{38} clusters; meanwhile, as shown in Fig. 10(d), on the $Pd_sPd_{sub}Cu_{36}$-I cluster, the electron mainly accumulated in the area of Pd ensemble; Further, the charges of outer shell Pd atom (-0.196 *e*) and its joint inner shell Pd atom (0.052 *e*) show that the charge transfer from the inner shell Pd to the outer shell Pd atom is more than that of the single Cu_{38} and Pd_{38} clusters. As a result, $Pd_sPd_{sub}Cu_{36}$-I cluster shows excellent catalytic activity toward C_2H_4 formation than the single Cu_{38} and Pd_{38} clusters.

On the Pd-modified Cu_{55} clusters, the charge of Pd atom on the outer shell of $Pd_sPd_{sub}Cu_{53}$-II cluster is -0.213 *e*, which is more negative than that of Cu and Pd atoms for the single Cu_{55} and Pd_{55} clusters (-0.023 and -0.095 *e*, respectively). However, as shown in Fig. 10(f)–(h), the charge density of Pd ensemble is weaker than that of Cu-Cu and Pd-Pd atoms for the single Cu_{55} and Pd_{55} clusters, respectively. Thus, the $Pd_sPd_{sub}Cu_{53}$-II cluster exhibits poor catalytic activity compared to the single Cu_{55} and Pd_{55} clusters.

4. Conclusions

In this work, C_2H_2 selective hydrogenation on a series of Pd-modified Cu nano-cluster catalysts have been investigated to examine the effects of Pd promoter, its ensemble and cluster size on the C_2H_4

selectivity and activity by DFT calculations. The results show that Pd-modified Cu_{13} and Cu_{55} clusters shows lower C_2H_4 selectivity and activity, however, only when Cu catalyst has a moderate size such as Cu_{38} cluster, Pd ensemble composed of outer shell and its contiguous inner-layer Pd atoms can significantly enhance C_2H_4 selectivity and activity, which is attributed to the more negative charges on the shell Pd atom as the active center for C_2H_2 selective hydrogenation. While the individual Pd atom replacing the outer shell Cu atom cannot improve the catalytic performance. Thus, controlling the size of Cu catalyst at a moderate size, followed by introducing Pd into Cu catalyst to form Pd ensemble composed of inner shell and its contiguous inner shell Pd atoms is an efficient way to improve the catalytic performance of C_2H_2 selective hydrogenation.

Acknowledgment

This work is financially supported by the Key projects of National Natural Science Foundation of China (No. 21736007), National Natural Science Foundation of China (No. 21776193) and the Top Young Innovative Talents of Shanxi.

Appendix A. Supplementary data

The detailed descriptions about all the possible adsorption configuration of C_2H_x (x = 2–5) species, the structures of initial, transition, final states of all reactions involving in the selective hydrogenation of C_2H_2 over the $Pd_sPd_{sub}Cu_{36}$-I, the single Cu_{55} and the $Pd_sPd_{sub}Cu_{53}$-II clusters, as well as the details of two-step model for C_2H_4 formation have been presented. Supplementary data to this article can be found online at https://doi.org/10.1016/j.apsusc.2019.03.006.

References

[1] T.V. Choudhary, C. Sivadinarayana, A.K. Datye, D. Kumar, D.W. Goodman, Acetylene hydrogenation on Au-based catalysts, Catal. Lett. 86 (2003) 1–8.
[2] F. Studt, P.F. Abild, T. Bligaard, R.Z. Sørensen, C.H. Christensen, J.K. Nørskov, On the role of surface modifications of palladium catalysts in the selective hydrogenation of acetylene, Angew. Chem. Int. Ed. 47 (2010) 9299–9302.
[3] J. Panpranot, K. Kontapakdee, P. Praserthdam, Selective hydrogenation of acetylene in excess ethylene on micron-sized and nanocrystalline TiO_2 supported Pd catalysts, Appl. Catal. A Gen. 314 (2006) 128–133.
[4] G.X. Pei, X.Y. Liu, A.Q. Wang, A.F. Lee, M.A. Isaacs, L. Li, X.L. Pan, X.F. Yang, X.D. Wang, Z. Tai, K. Wilson, T. Zhang, Ag alloyed Pd single-atom catalysts for efficient selective hydrogenation of acetylene to ethylene in excess ethylene, ACS Catal. 5 (2015) 3717–3725.
[5] A. Borodzinski, G. Bond, Selective hydrogenation of ethyne in ethene-rich streams on palladium catalysts. Part 1. Effect of changes to the catalyst during reaction, Catal. Rev. 48 (2006) 91–144.
[6] A. Borodziński, G.C. Bond, Selective hydrogenation of ethyne in ethene-rich streams on palladium catalysts, part 2: steady-state kinetics and effects of palladium particle size, carbon monoxide, and promoters, Catal. Rev. 50 (2008) 379–469.
[7] W.T. Mcgown, C. Kemball, D.A. Whan, M.S. Scurrell, Hydrogenation of acetylene in excess ethylene on an alumina supported palladium catalyst in a static system, J. Chem. Soc. Faraday Trans. 73 (1977) 632–647.
[8] W. Huang, J.R. Mccormick, R.F. Lobo, J.G. Chen, Selective hydrogenation of acetylene in the presence of ethylene on zeolite-supported bimetallic catalysts, J. Catal. 246 (2007) 40–51.
[9] M.R. Rahimpour, O. Dehghani, M.R. Gholipour, M.S.S. Yancheshmeh, S.S. Haghighi, A. Shariati, A novel configuration for Pd/Ag/α-Al_2O_3 catalyst regeneration in the acetylene hydrogenation reactor of a multifeed cracker, Chem. Eng. J. 198–199 (2012) 491–502.
[10] D. Mei, M. Neurock, C.M. Smith, Hydrogenation of acetylene–ethylene mixtures over Pd and Pd–Ag alloys: first-principles-based kinetic Monte Carlo simulations, J. Catal. 268 (2009) 181–195.
[11] S.K. Kim, C. Kim, H.L. Ji, J. Kim, H. Lee, H.M. Sang, Performance of shape-controlled Pd nanoparticles in the selective hydrogenation of acetylene, J. Catal. 306 (2013) 146–154.
[12] A.D. Benavidez, P.D. Burton, J.L. Nogales, A.R. Jenkins, S.A. Ivanov, J.T. Miller, A.M. Karim, A.K. Datye, Improved selectivity of carbon-supported palladium catalysts for the hydrogenation of acetylene in excess ethylene, Appl. Catal. A Gen. 482 (2014) 108–115.
[13] P. Praserthdam, B. Ngamsom, N. Bogdanchikova, S. Phatanasri, M. Pramotthana, Effect of the pretreatment with oxygen and/or oxygen-containing compounds on the catalytic performance of Pd-Ag/Al_2O_3 for acetylene hydrogenation, Appl. Catal. A Gen. 230 (2002) 41–51.
[14] B. Ngamsom, N. Bogdanchikova, M.A. Borja, P. Praserthdam, Characterisations of Pd-Ag/Al_2O_3 catalysts for selective acetylene hydrogenation: effect of pretreatment with NO and N_2O, Catal. Commun. 5 (2004) 243–248.
[15] A. Sarkany, Z. Zsoldos, G.J. Stefler, W. Hightower, L. Guczi, Promoter effect of Pd in hydrogenation of 1, 3-butadiene over Co-Pd catalysts, J. Catal. 157 (1995) 179–189.
[16] W.G. Menezes, L. Altmann, V. Zielasek, K. Thiel, M. Bäumer, Bimetallic Co-Pd catalysts: study of preparation methods and their influence on the selective hydrogenation of acetylene, J. Catal. 300 (2013) 125–135.
[17] A.J. Mccue, C.J. Mcritchie, A.M. Shepherd, J.A. Anderson, Cu/Al_2O_3 catalysts modified with Pd for selective acetylene hydrogenation, J. Catal. 319 (2014) 127–135.
[18] B. Bridier, N. López, J. Pérez-Ramírez, Partial hydrogenation of propyne over copper-based catalysts and comparison with nickel-based analogues, J. Catal. 269 (2010) 80–92.
[19] B. Bridier, M.A.G. Hevia, N. López, J. Pérez-Ramírez, Permanent alkene selectivity enhancement in copper-catalyzed propyne hydrogenation by temporary CO supply, J. Catal. 278 (2011) 167–172.
[20] S. Leviness, V. Nair, A.H. Weiss, Z. Schay, L. Guczi, Acetylene hydrogenation selectivity control on PdCu/Al_2O_3 catalysts, J. Mol. Catal. 25 (1984) 131–140.
[21] S. Abelló, D. Verboekend, B. Bridier, J. Pérez-Ramírez, Activated takovite catalysts for partial hydrogenation of ethyne, propyne, and propadiene, J. Catal. 259 (2008) 85–95.
[22] D.L. Trimm, I.O.Y. Liu, N.W. Cant, The selective hydrogenation of acetylene over a Ni/SiO_2 catalyst in the presence and absence of carbon monoxide, Appl. Catal. A Gen. 374 (2010) 58–64.
[23] D.L. Trimm, N.W. Cant, I.O.Y. Liu, The selective hydrogenation of acetylene in the presence of carbon monoxide over Ni and Ni-Zn supported on $MgAl_2O_4$, Catal. Today 178 (2011) 181–186.
[24] G. Kyriakou, M.B. Boucher, A.D. Jewell, E.A. Lewis, T.J. Lawton, A.E. Baber, H.L. Tierney, M. Flytzani-Stephanopoulos, E.C.H. Sykes, Isolated metal atom geometries as a strategy for selective heterogeneous hydrogenations, Science. 335 (2012) 1209–1212.
[25] H.L. Tierney, A.E. Baber, J.R. Kitchin, E.C. Sykes, Hydrogen dissociation and spillover on individual isolated palladium atoms, Phys. Rev. Lett. 103 (2009) 246102–246106.
[26] S.K. Kim, J.H. Lee, I.Y. Ahn, W.J. Kim, S.H. Moon, Performance of Cu-promoted Pd catalysts prepared by adding Cu using a surface redox method in acetylene hydrogenation, Appl. Catal. A Gen. 401 (2011) 12–19.
[27] R.G. Zhang, B. Zhao, L.L. He, A.J. Wang, B.J. Wang, Cost-effective promoter-doped Cu-based bimetallic catalysts for the selective hydrogenation of C_2H_2 to C_2H_4: the effect of the promoter on selectivity and activity, Phys. Chem. Chem. Phys. 20 (2018) 17487–17496.
[28] R.G. Zhang, B. Zhao, L.X. Ling, A.J. Wang, C.K. Russell, B.J. Wang, M.H. Fan, A cost-effective Pd-doped Cu bimetallic materials to tuning selectivity and activity using doped atom ensembles as active sites for efficient removal of acetylene from ethylene, Chem. Cat. Chem. 10 (2018) 2424–2432.
[29] J.T. Wehrli, D.J. Thomas, M.S. Wainwright, D.L. Trimm, N.W. Cant, Selective hydrogenation of C_4-acetylenes over an ion-exchanged copper on silica catalyst, Appl. Catal. 66 (1990) 199–208.
[30] M.R. Stammbach, D.J. Thomas, D.L. Trimm, M.S. Wainwright, Hydrogenation of ethyne over an ion-exchanged copper on silica catalyst, Appl. Catal. 58 (1990) 209–217.
[31] X.J. Liu, D.X. Tian, C.G. Meng, DFT study on the adsorption and dissociation of H_2 on Pd_n (n = 4, 6, 13, 19, 55) clusters, J. Mol. Struct. 1080 (2015) 105–110.
[32] A. Karelovic, P. Ruiz, The role of copper particle size in low pressure methanol synthesis via CO_2 hydrogenation over Cu/ZnO catalysts, Catal. Sci. Technol. 5 (2015) 869–881.
[33] Z.J. Zuo, L. Wang, P.D. Han, W. Huang, Insight into the size effect on methanol decomposition over Cu-based catalysts based on density functional theory, Comput. Theor. Chem. 1033 (2014) 14–22.
[34] R.G. Zhang, T. Duan, B.J. Wang, L.X. Ling, Unraveling the role of support surface hydroxyls and its effect on the selectivity of C_2 species over Rh/γ-Al_2O_3 catalyst in syngas conversion: a theoretical study, Appl. Surf. Sci. 379 (2016) 384–394.
[35] B. Zhao, R.G. Zhang, Z.X. Huang, B.J. Wang, Effect of the size of Cu clusters on selectivity and activity of acetylene selective hydrogenation, Appl. Catal. A Gen. 546 (2017) 111–121.
[36] A.B. Aaen, E. Lægsgaard, A.V. Ruban, I. Stensgaard, Submonolayer growth of Pd on Cu(111) studied by scanning tunneling microscopy, Surf. Sci. 408 (1998) 43–56.
[37] T. Duan, R.G. Zhang, L.X. Ling, B.J. Wang, Insights into the effect of Pt atomic ensemble on HCOOH oxidation over Pt-decorated Au bimetallic catalyst to maximize Pt utilization, J. Phys. Chem. C 120 (2016) 2234–2246.
[38] D.W. Yuan, Z.R. Liu, Atomic ensemble effects on formic acid oxidation on PdAu electrode studied by first-principles calculations, J. Power Sources 224 (2013) 241–249.
[39] Q. Fu, Y. Luo, Active sites of Pd-doped flat and stepped Cu(111) surfaces for H_2 dissociation in heterogeneous catalytic hydrogenation, ACS Catal. 3 (2013) 1245–1252.
[40] B. Delley, An all-electron numerical method for solving the local density functional for polyatomic molecules, J. Chem. Phys. 92 (1990) 508–517.
[41] B. Delley, From molecules to solids with the $Dmol^3$ approach, J. Chem. Phys. 113 (2000) 7756–7764.
[42] D.X. Tian, H.L. Zhang, J.J. Zhao, Structure and structural evolution of Ag_n(n = 3-22) clusters using a genetic algorithm and density functional theory method, Solid State Commun. 144 (2007) 174–179.
[43] J.P. Perdew, K. Burke, M. Ernzerhof, J.P. Perdew, K. Burke, M. Ernzerhof,

Generalized gradient approximation made simple, Phys. Rev. Lett. 77 (1996) 3865–3868.
[44] M. Dolg, U. Wedig, H. Stoll, H. Preuss, Efficiency of numerical basis sets for predicting the binding energies of hydrogen bonded complexes: evidence of small basis set superposition error compared to Gaussian basis sets, J. Chem. Phys. 86 (1987) 866–872.
[45] T.A. Halgren, W.N. Lipscomb, The synchronous-transit method for determining reaction pathways and locating molecular transition states, Chem. Phys. Lett. 49 (1977) 225–232.
[46] N. Govind, M. Petersen, G. Fitzgerald, D. King-Smith, J. Andzelm, A generalized synchronous transit method for transition state location, Comput. Mater. Sci. 28 (2003) 250–258.
[47] C.G. Varejão, Influence of surface structures, subsurface carbon and hydrogen, and surface alloying on the activity and selectivity of acetylene hydrogenation on Pd surfaces: a density functional theory study, J. Catal. 305 (2013) 264–276.
[48] B. Yang, R. Burch, C. Hardacre, P. Hu, P. Hughes, Mechanistic study of 1,3-butadiene formation in acetylene hydrogenation over the Pd-based catalysts using density functional calculations, J. Phys. Chem. C 118 (2014) 1560–1567.
[49] R.G. Zhang, J. Zhang, Z. Jiang, B.J. Wang, M.H. Fan, The cost-effective Cu-based catalysts for the efficient removal of acetylene from ethylene: the effects of Cu valence state, surface structure and surface alloying on the selectivity and activity, Chem. Eng. J. 351 (2018) 732–746.
[50] E. Fernández, M. Boronat, A. Corma, Trends in the reactivity of molecular O_2 with copper clusters: influence of size and shape, J. Phys. Chem. C 119 (2015) 19832–19846.
[51] K. Shin, H.K. Da, C.Y. Sang, H.M. Lee, Structural stability of AgCu bimetallic nanoparticles and their application as a catalyst: a DFT study, Catal. Today 185 (2012) 94–98.
[52] S. Darby, T.V. Mortimerjones, R.L. Johnston, C. Roberts, Theoretical study of Cu–Au nanoalloy clusters using a genetic algorithm, J. Chem. Phys. 116 (2002) 1536–1550.
[53] M. Kabir, A. Mookerjee, A.K. Bhattacharya, Structure and stability of copper clusters: a tight-binding molecular dynamics study, Phys. Rev. A 69 (2004) 361–367.
[54] Y. Yang, J. Evans, J.A. Rodriguez, M.G. White, P. Liu, Fundamental studies of methanol synthesis from CO_2 hydrogenation on Cu(111), Cu clusters, and Cu/ZnO (0001), Phys. Chem. Chem. Phys. 12 (2010) 9909–9917.
[55] I.A. Hijazi, Y.H. Park, Structure of pure metallic nanoclusters: Monte Carlo simulation and ab initio study, Eur. Phys. J. D. 59 (2010) 215–221.
[56] M. Itoh, V. Kumar, T. Adschiri, Y. Kawazoe, Comprehensive study of sodium, copper, and silver clusters over a wide range of sizes $2 \le N \le 75$, J. Chem. Phys. 131 (2009) 2141–2161.
[57] Y.H. Park, I.A. Hijazi, Critical size of transitional copper clusters for ground state structure determination: empirical and ab initio study, Mol. Simul. 38 (2012) 241–247.
[58] U. Lammers, G. Borstel, Electronic and atomic structure of copper clusters, Phys. Rev. B: Condens. Matter Mater. Phys. 49 (1994) 17360–17377.
[59] L. Zhang, W. Li, Molecular dynamics investigation to indicate facet effects on coalescence processes of two copper clusters with different structures, Comput. Mater. Sci. 51 (2012) 91–95.
[60] F. Baletto, R. Ferrando, Structural properties of nanoclusters: energetic, thermodynamic, and kinetic effects, Rev. Mod. Phys. 77 (2005) 371–423.
[61] H.F. Gong, W. Lu, L.M. Wang, G.P. Li, S.X. Zhang, The effect of deposition velocity and cluster size on thin film growth by Cu cluster deposition, Compt. Mater. Sci. 65 (2012) 230–234.
[62] X.X. Cao, A. Mirjalili, J. Wheeler, W.T. Xie, B.W.L. Jang, Investigation of the preparation methodologies of Pd-Cu single atom alloy catalysts for selective hydrogenation of acetylene, Front. Chem. Sci. Eng. 9 (2015) 442–449.
[63] Y.J. Chen, J.X. Chen, Selective hydrogenation of acetylene on SiO_2 supported Ni-In bimetallic catalysts: promotional effect of In, Appl. Surf. Sci. 387 (2016) 16–27.
[64] X.M. Cao, R. Burch, C. Hardacre, P. Hu, An understanding of chemoselective hydrogenation on crotonaldehyde over Pt(111) in the free energy landscape: the microkinetics study based on first-principles calculations, Catal. Today 165 (2011) 71–79.
[65] B. Yang, D. Wang, X.Q. Gong, P. Hu, Acrolein hydrogenation on Pt(211) and Au (211) surfaces: a density functional theory study, Phys. Chem. Chem. Phys. 13 (2011) 21146–21152.
[66] L. Xu, E.E. Stangland, M. Mavrikakis, Ethylene versus ethane: a DFT-based selectivity descriptor for efficient catalyst screening, J. Catal. 362 (2018) 18–24.
[67] J. Cheng, P. Hu, Theory of the kinetics of chemical potentials in heterogeneous catalysis, Angew. Chem. Int. Ed. 50 (2011) 7650–7654.
[68] J. Cheng, P. Hu, P. Ellis, S. French, G. Kelly, M.C. Lok, Brønsted-Evans-Polanyi relation of multistep reactions and volcano curve in heterogeneous catalysis, J. Phys. Chem. C 112 (2008) 1308–1311.
[69] J.W. Carneiro, M.T. Cruz, Density functional theory study of the adsorption of formaldehyde on Pd_4 and on Pd_4/γ-Al_2O_3 clusters, J. Phys. Chem. A 112 (2008) 8929–8937.
[70] Y. Han, M. Zhang, W. Li, J.L. Zhang, Effect of TiO_2 support on the structural and electronic properties of Pd_mAg_n clusters: a first-principles study, Phys. Chem. Chem. Phys. 14 (2012) 8683–8692.
[71] H.T. Wang, L.J. Chen, Y.K. Lv, R.P. Ren, H_2 dissociation on γ-Al_2O_3 supported Cu/Pd atoms: a DFT investigation, Appl. Surf. Sci. 290 (2014) 154–160.
[72] H. Chen, J.Q. Yue, Y.Y. Li, C.H. Yi, B.L. Yang, S.T. Qi, Catalytic activity prediction of different metal surfaces for N_2O catalytic decomposition by density functional theory, Comput. Theor. Chem. 1057 (2015) 1–6.